Biosensors and Bioelectronics 42 (2013) 214–218

Contents lists available at SciVerse ScienceDirect

Biosensors and Bioelectronics

journal homepage: www.elsevier.com/locate/bios

Sensitive and selective detection of biothiols based on target-induced agglomeration of silver nanoclusters

Na Zhang, Fei Qu, Hong Qun Luo*, Nian Bing Li*

Key Laboratory of Eco-environments in Three Gorges Reservoir Region (Ministry of Education), School of Chemistry and Chemical Engineering, Southwest University, Chongqing 400715, PR China

ARTICLE INFO

Article history:
Received 31 July 2012
Received in revised form
20 October 2012
Accepted 26 October 2012
Available online 5 November 2012

Keywords:
Silver nanoclusters
Biothiols
Agglomeration
Fluorescence quenching

ABSTRACT

In this work, we present a label-free biosensor for the sensing of biothiols such as cysteine, homocysteine, and glutathione. This biosensor is based on the fluorescent probe, polyethyleneimine-capped silver nanoclusters. The selective binding of silver nanoclusters to biothiols promotes the silver nanoclusters agglomeration to yield larger non-fluorescent silver nanoparticles. And the fluorescence intensity of silver nanoclusters was quenched efficiently with increasing concentration of biothiols. The other amino acids introduced to the silver nanoclusters probe solution did not quench the fluorescence of the probe as they do not have thiol group which has strong affinity to the silver nanoclusters. Thus, this biosensor allowed selectively investigation of biothiols. The as-proposed biosensor was sensitive for the detection of biothiols. The linear ranges for cysteine, homocysteine, and glutathione were 0.1–10 μM (R^2=0.9930), 0.1–10 μM (R^2=0.9924), and 0.5–6 μM (R^2=0.9900), respectively. The detection limits for cysteine, homocysteine, glutathione were 42, 47, and 380 nM, respectively. The silver nanoclusters-based fluorescent biosensor provides a simple, cost-effective, and sensitive platform for the detection of biothiols.

1. Introduction

Varied concentrations of biothiols such as cysteine (Cys), homocysteine (Hcy), and glutathione (GSH) play a crucial role in our human health (Wood et al., 2003). Biothiols are a class of mercaptan having a sulfhydryl functional group and are among the most significant antioxidants against oxidative damage which leads potentially to disease (Wlodek, 2002). Cys deficiency is implicated in many syndromes such as slow growth in children, skin lesions, hair depigmentation, liver damage, and edema (Shahrokhian, 2001). An elevated level of Hcy has been associated with an increased risk of Alzheimer's disease, cardiovascular disease, inflammatory bowel disease, and osteoporosis (Refsum et al., 1998; Seshadri et al., 2002). The tripeptide GSH (γ-Glu–Cys–Gly) is the most abundant biothiol species in cells and typically associated with beneficial antioxidant activity which protects against oxidative damage and helps to trap free radical that can damage DNA and RNA (Hong et al., 2006). Thus, sensitive and selective determination of these biothiols is highly required. The current procedures for identification or quantification of thiol compounds in real samples are slightly different. Human plasma samples (Shiu et al., 2011; Gao et al., 2011; Bistra et al., 2008) and human urine samples (Xu et al., 2012) need the reduction of disulfide to free thiols, and plasma samples also need to precipitate proteins after reduction. Cell samples (Han et al., 2009; Zhang et al., 2009) are harvested after trypsin digestion and cell lysis. Up to now, among the different methods to detect and quantify the biothiols (Huang and Chang, 2006; Lu et al., 2007; Moore et al., 2004; Ruzi-Díaz et al., 2006; Shahrokhian and Karimi, 2004), optical techniques are more desirable since they are easy to operate, sensitive, and efficient (Han et al., 2009; Han and Wang, 2011; Ruan et al., 2010; Sun et al., 2011; Wang et al., 2012; Xu et al., 2012; Zhang et al., 2009).

Few-atom fluorescent silver nanoclusters (AgNCs) as a new class of fluorescent probes (Zheng et al., 2007) have received widespread attention in chemical and biological detection applications owing to their special properties like small size, photostability, biocompatibility, water solubility, high emission rates, and large Stokes shift (Vosch et al., 2007). These merits make AgNCs good candidates as fluorophores for biological labeling. Thiols-induced fluorescence quenching or enhancement of AgNCs has been studied widely which demonstrates immense potential in the detection of thiols. For example, a signal-on assay for thiol compounds by DNA-templated AgNCs (Huang et al., 2011) and a signal-off assay for Cys by poly (methacrylic acid)-templated AgNCs (Shang and Dong, 2009) have been reported.

Herein, we report on an AgNCs-based fluorescent probe which was capped by polyethyleneimine (PEI), a water-soluble polymer

* Corresponding authors. Tel./fax: +86 23 6825 3237.
E-mail addresses: luohq@swu.edu.cn (H.Q. Luo), linb@swu.edu.cn (N.B. Li).

0956-5663/$ - see front matter © 2012 Elsevier B.V. All rights reserved.
http://dx.doi.org/10.1016/j.bios.2012.10.090

with lots of amino groups, for the detection of biothiols such as Cys, Hcy, and GSH in aqueous solution. The fluorescence of the PEI-capped AgNCs was quenched efficiently in the presence of biothiols. This assay for biothiols was not only sensitive and selective but also simple, cost-effective, and environmentally friendly.

2. Material and methods

2.1. Chemicals and materials

Silver nitrate ($AgNO_3$, 99%) and beta mercaptoethanol (ME) were obtained from Shanghai Shenbo Chemical Co., Ltd. (Shanghai, China). Branched polyethyleneimine (PEI) (Mw=10,000, 99%), L-cysteine (Cys, >99%), L-homocysteine (Hcy, >95%), L-glutathione (GSH, reduced, >98%), other amino acids, 4-(2-hydroxyethyl)-1-piperazineethanesulfonic acid (HEPES), and tris-(hydroxymethyl) aminomethane (Tris), and bovine serum albumin (BSA) were purchased from Aladdin Chemistry Co., Ltd. (China). Tris-(2-carboxyethyl) phosphine hydrochloride (TCEP) and dithiothreitol (DTT) were purchased from Sigma-Aldrich Chemical Co. (USA). All the reagents were of analytical reagent grade and were used as received. All solutions were freshly prepared before use. Milli-Q ultrapure water (18.2 MΩ cm) was used in all experiments.

2.2. Instrumentation

The AgNCs were characterized by transmission electron microscopy (TEM) on a Hitachi 7500 transmission electron microscope (Hitachi, Japan) with an accelerating voltage of 80 KV. The samples for TEM were obtained by drying sample droplets from water onto a 300-mesh Cu grid coated with a lacey carbon film. The fluorescence measurements were performed on an F-2700 fluorescence spectrophotometer (Hitachi, Japan) with a quartz cell (1 cm × 1 cm). The slit widths were 10 and 10 nm for excitation and emission and the photomultiplier tube voltage was set at −400 V. The UV–vis absorption spectra were recorded on a UV-2450 spectrophotometer (Shimadzu, Japan). The Fourier transform infrared spectra were taken with a Bruker IFS (Germany) 113v spectrometer after pelleting the fine powder with KBr. Zeta potentials were performed by laser Doppler electrophoresis using a Zetasizer Nano ZS (Malvern Instruments Ltd., U.K.).

2.3. Preparation of polyethyleneimine-capped fluorescent silver nanoclusters

The PEI-capped fluorescent silver nanoclusters were synthesized according to a one-pot method with slight modification. Briefly, PEI (100 μL, 0.2 M) and HEPES (50 μL, 1 mM) were added to 95 μL of aqueous solution, and homogenized under stirring for 2 min. Then $AgNO_3$ (250 μL, 0.1 M) was added to the previous solution and blended under stirring for 2 min. At last, formaldehyde solution (5 μL, 37%–40%) was added and homogenized under stirring for 2 min. The colloidal silver solution was heated in water bath at 70 °C for 10 min. Thus, the stable solution of PEI-capped AgNCs was obtained for further use. The as-prepared PEI-capped AgNCs were stable for at least 1 month.

2.4. Preparation of real samples

Fresh human blood samples were obtained from the local hospital. The conversion of disulfides to free thiols was conducted by treating the plasma sample with a reducing reagent, TCEP, according to the literature procedure (Bistra et al., 2008; Huang et al., 2011). Typically, to 400 μL of plasma sample 40 μL of TCEP (35 mM) was added. The sample was incubated at 40 °C for 10 min and 400 μL of precipitation agent acetonitrile was added, followed by centrifugation at 3000 rpm for 20 min. The supernatant which contained biothiols in plasma was used for further analysis.

2.5. Detection of cysteine, homocysteine, and glutathione

Mixtures (500 μL) of the PEI-capped AgNCs (30 μL, 0.01 C), boric acid–borax buffer (150 μL, 20 mM, pH 8.2), and biothiols (Cys, Hcy, GSH, 0–80 μM) were equilibrated at ambient temperature for 30 min. Subsequently, the mixtures were subjected to fluorescence measurement with excitation at 375 nm. All experiments were performed in triplicate.

Note: Due to the lack of the concentration information of AgNCs at present, we denote the concentration of the as-prepared AgNCs as "1C". The concentration of AgNCs in characterization experiments (ultimate concentration, 0.01C) was higher than those of the optimization and detection procedures.

3. Results and discussion

3.1. Characterization of the polyethyleneimine-capped silver nanoclusters

It has been demonstrated that the properties of the nanoclusters are prominently influenced by the template molecules used for nanoclusters synthesis (Xu and Suslick, 2010). In this paper, AgNCs were synthesized according to a modified one-pot method (Manoth et al., 2009) based on a PEI-modified silver mirror reaction which silver ions interacted with the amino groups of PEI. The cationic polymer, branched PEI, has been used widely as a gold standard for gene delivery vehicle as it is nontoxic, biodegradable, cell-specific, and non-immunogenic (Kim et al., 2011). This suggests that PEI-capped AgNCs can also be used in the fields of medicine and biology. The as-prepared water-soluble PEI-capped AgNCs displayed a yellow color, and showed a strongly blue fluorescence under the UV-lamp (λ=365 nm). The PEI-capped AgNCs showed a high fluorescence quantum yield of 3.81% in ethanol calculated by use of quinine sulfate in 0.1 M H_2SO_4 as a reference chromophore (Fletcher, 1969) and were very stable for at least 1 month without any obvious colloidal aggregation. The synthesized PEI-capped AgNCs exhibited an average diameter of ~2 nm (Fig. 1a), an intense absorption band at 354 nm in the ultraviolet range, and an emission at 455 nm when excited at 375 nm. However, it is well-known that branched PEI also emits light in the blue region. In order to confirm the formation of AgNCs, we have performed the following experiments. First, we compared the fluorescence spectrum of PEI alone with that of PEI-capped AgNCs. We found that PEI and AgNCs had similar excitation and emission spectra, but the fluorescence intensity of PEI was very weak. In Fig. S1, the concentration of PEI alone is 500-fold higher than that of PEI contained in AgNCs. And the absorption spectrum of PEI alone is different from that of AgNCs. Then, we checked whether the fluorescence was from PEI oxidized by formaldehyde. We synthesized contrast solution without adding silver nitrate according to the process of AgNCs synthesis. From the results we confirmed the formation of AgNCs because the fluorescence intensity and absorbance of the contrast solution were extremely weak compared with those of PEI-capped AgNCs at the same PEI concentration (Fig. S2).

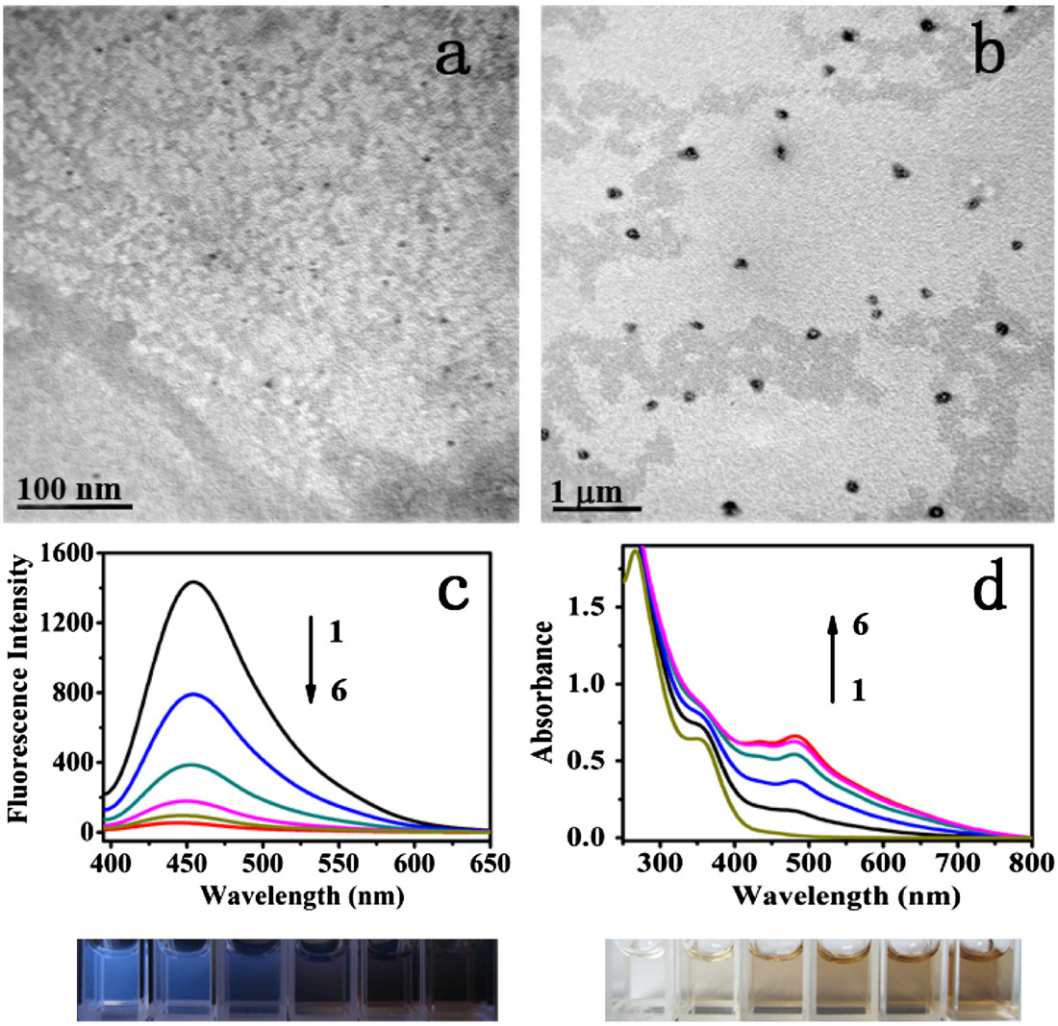

Fig. 1. TEM images of PEI-capped AgNCs (a) and PEI-capped AgNCs upon addition of 300 μM Cys (b). (c) Fluorescence spectra of the PEI-capped AgNCs in the presence of different concentrations of Cys (from 1 to 6: 0, 100, 200, 300, 400, 500 μM). The pictures below represent the fluorescence change of the relevant solutions under the UV lamp. (d) UV–vis absorption spectra of the PEI-capped AgNCs in the presence of various concentrations of Cys (from 1 to 6: 0, 100, 200, 300, 400, 500 μM). The photos below show the color change of the relevant solutions. (For interpretation of the references to color in this figure legend, the reader is referred to the web version of this article.)

3.2. *Thiol-induced fluorescence quenching of the PEI-capped AgNCs*

The AgNCs were protected stably by the PEI template. Once biothiols (Cys, Hcy, and GSH) were added to the AgNCs solution, the fluorescence intensity of PEI-capped AgNCs at 455 nm was greatly quenched and the quenching effects were enhanced with increasing concentration of biothiols (Fig. 1c). Previous study demonstrated that nucleophilic reagents could be chemisorbed on the surface of AgNCs and promoted the agglomeration of clusters to yield larger particles (Henglein et al., 1991a,b). Herein, we proposed that such chemisorption and agglomeration also took place on PEI-capped AgNCs when the biothiols were added. Silver atoms have low-lying vacant d orbitals, and electron pairs from the nucleophile can enter vacant electron orbitals on the silver atoms (Mulvaney et al., 1991). Biothiols as a nucleophile interacted with the PEI-capped AgNCs and were then adsorbed on the surface of AgNCs. In consequence of electron donation, PEI-capped AgNCs experienced changes in clusters agglomeration and surface charge in solution over time. The adsorbed biothiols on the AgNCs would break the AgNCs–PEI bond and neutralize AgNCs surface charge. As a consequence, the increased van der Waals attractive force among these detached biothiols-coated AgNCs drove the clusters agglomeration, leading to the formation of larger silver nanoparticles. Here, we studied the effect of biothiols on the PEI-capped AgNCs using Cys as a model. The diluted solution of AgNCs was nearly colorless. When Cys was added, the color of this solution changed to brown-red immediately. And a new absorption peak appeared at 480 nm (Fig. 1d), indicating that Cys was adsorbed on the PEI-capped AgNCs. IR spectral data also supported the chemisorption of Cys on AgNCs in that the stretching band of S–H of free Cys at 2550 cm^{-1} disappeared when Cys was added to the AgNCs solution (Fig. S3). The zeta potential of the AgNCs probe solution decreased with increasing Cys concentration, which indicated that Cys was adsorbed on AgNCs, leading to decrease in the surface charge of AgNCs (Fig. S4). It is clearly seen that the absorbance was highly dependent on the quantity of Cys added. The new absorption peak at 480 nm became more intense with increasing concentration of Cys. When more Cys was added to the AgNCs solution, another absorption peak at 430 nm also appeared. The appearance of the new absorption band indicated the change in the size or shape of AgNCs (Cheng et al., 2003). Evidences from TEM images, which correlate with the absorption spectral observations, also indicate the chemisorption of Cys on the AgNCs and the formation of larger size nanoparticles as shown in Fig. 1(b). The as-prepared AgNCs were monodispersed with an average diameter of 2 nm and well separated. When Cys was added, the TEM images showed the agglomeration of AgNCs. The formed larger silver nanoparticles exhibited an average diameter of 110 nm and various geometries (Fig. S5). These experimental results revealed that the

reaction mechanism did not originate from the formation of the non-fluorescent ground-state complex (Huang et al., 2011) or Hcy-involved assembling of AgNCs (Sun et al., 2011), but from thiol-induced agglomeration of the AgNCs as given in Scheme 1. Biothiols chemisorbed on PEI-capped AgNCs freed the AgNCs and lowered the surface charge, and then the detached clusters reacted with each other to form large non-fluorescent nanoparticles.

3.3. Optimization of factors affecting the detection of biothiols

In this system, several factors that may affect the quenching efficiency of the AgNCs–biothiols were optimized, such as the concentration of AgNCs, pH value, buffer system, and reaction time. The concentration of AgNCs not only affected the background fluorescence intensity of the probe solution, but also influenced the sensitivity of this method for the determination of biothiols. Fig. S6 indicates that the lower the probe concentration is, the higher the quenching efficiency becomes. Considering the background signals of probe, we chose 30 μL of AgNCs (0.01C) as the optimum amount of the probe.

The effect of pH on the fluorescence intensity was investigated as pH affected the charge characters of the amino groups of PEI and $-NH_2$, –COOH, and –SH groups of biothiols. Britton–Robinson (BR) buffer covers the wide pH range from 1.81 to 11.92, which was used for pH screening test. The fluorescence intensities of PEI-capped AgNCs in the absence and presence of Cys were all enhanced with increasing pH and then reached stable. The quenching efficiency also reached a maximum value and kept constant (Fig. S7). In alkaline environment, there were no electrostatic repulsions among the amino groups of branched PEI as they were un-ionized forms. So the PEI-capped AgNCs were more stable when pH > 7. We also carefully tested the detection of thiol compounds using the AgNCs probe in different buffer systems (20 mM, pH 8.2), including BR, Tris-acetate, HEPES, and boric acid–borax. The values of $(I_{F0}-I_F)/I_{F0}$ for BR, Tris-acetate, HEPES, and boric acid–borax at 2 μM Cys were 15.9%, 15.6%, 16.7%, and 24.6%, respectively. Here, I_{F0} and I_F denote the fluorescence intensity in the absence and presence of the thiol compound, respectively. To obtain the maximal quenching efficiency, a 20 mM boric acid–borax buffer at pH 8.2 was used in our detection system.

When Cys was added to the AgNCs solution, the color of the solution changed immediately. In order to find a suitable reaction time for stabilizing the reaction solution, the effect of different reaction times on the fluorescence intensity of PEI-capped AgNCs in the presence of 2 μM Cys was tested. The results showed that the values of $(I_{F0}-I_F)/I_{F0}$ increased rapidly within 10 min and then the fluorescence intensity changed little over time. After 30 min, no significant change in the fluorescence intensity was found, as evidenced by the quenching of the fluorescence emission at 455 nm (Fig. S8). So 30 min of the reaction time was used in our detection system.

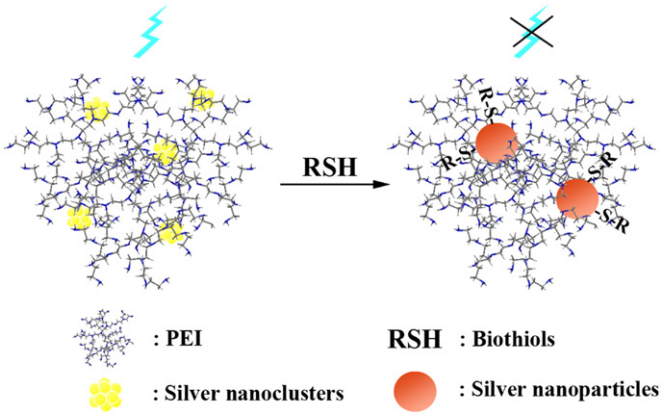

Scheme 1. Schematic illustration of the biothiols-induced agglomeration of PEI-capped AgNCs.

3.4. Sensitivity and selectivity of the silver nanoclusters for detection of biothiols

To estimate the sensitivity of the PEI-capped AgNCs for detecting biothiols, the fluorescence intensity at 455 nm was monitored as a function of the concentration of Cys, Hcy, and GSH, respectively. The fluorescence quenching factor $(I_{F0}-I_F)/I_{F0}$ was proportional to the concentration of biothiols. The linear ranges of fluorescence response of the sensor for Cys (Fig. 2), Hcy, and GSH (Fig. S9) were 0.1–10 μM ($R^2=0.9930$), 0.1–10 μM ($R^2=0.9924$), and 0.5–6 μM ($R^2=0.9900$), respectively. The detection limits for Cys, Hcy, and GSH were 42, 47, and 380 nM, respectively. The sensitivity of GSH was much lower than those of Cys and Hcy possibly because of steric effects that hindered the chemisorption of GSH on PEI-capped AgNCs. In addition, we have compared the detection limits and linear ranges of this method with those of the other methods reported to detect biothiols (Table S1). The proposed method was comparable to or better than others.

Under the optimum conditions, the fluorescence response of the PEI-capped AgNCs to various analytes showed good selectivity for Cys against other 19 amino acids at ten-fold higher concentration than Cys (Fig. 3). Only Cys caused decrease in the fluorescence intensity, revealing that the PEI-capped AgNCs probe was selective for Cys. To certify the performance of our assay for Cys detection in practical applications, the effect of the coexistence of Cys and ten-fold other

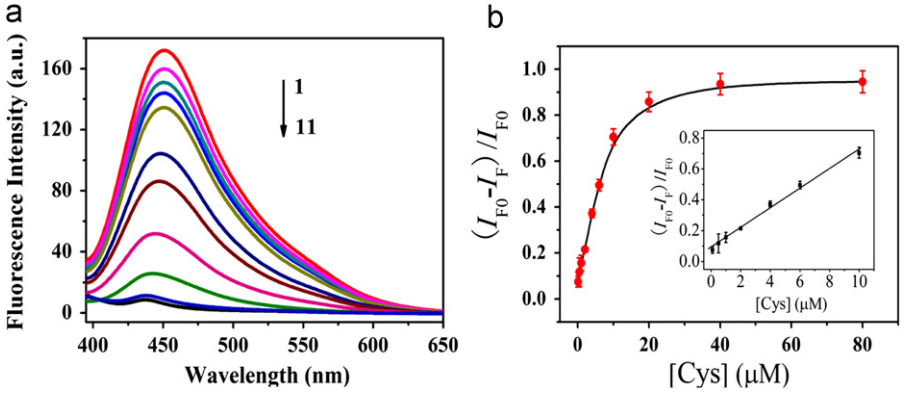

Fig. 2. (a) Fluorescence spectra of the PEI-capped AgNCs in the presence of increasing concentrations of Cys (from 1 to 11: 0–80 μM), (b) plot of the quenching factor $(I_{F0}-I_F)/I_{F0}$ at 455 nm versus the concentration of added Cys. Inset is the linear region for Cys.

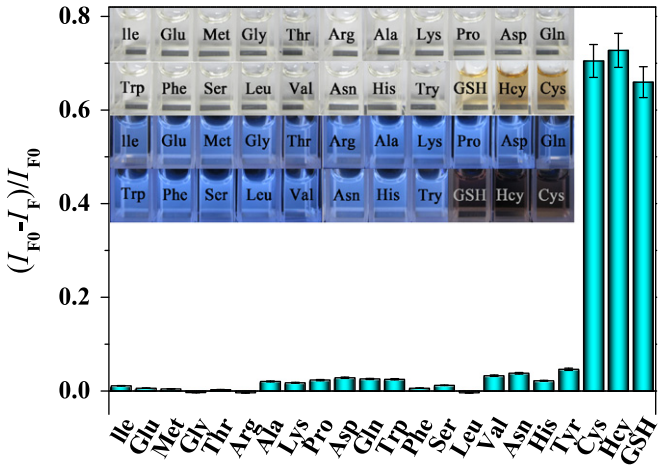

Fig. 3. The responses of different amino acids to PEI-capped AgNCs: Cys, Hcy and GSH (10 μM), other 19 amino acids (100 μM). The picture inserted shows the color and fluorescence change of AgNCs to different amino acids (300 μM). (For interpretation of the references to color in this figure legend, the reader is referred to the web version of this article.)

19 amino acids on the fluorescence response was investigated. The result suggested that the mixed amino acids caused little variation in fluorescence intensity compared with Cys alone. Hcy and GSH also showed good selectivity against other 19 amino acids as both of them contain a thiol group. These results indicated that the proposed assay had high selectivity for biothiols and it was practical for the detection of biothiols in biological samples.

3.5. Detecting biothiols in biological samples

As demonstrated above, the PEI-capped AgNCs probe exhibited good selectivity to Cys, Hcy, and GSH, which made the proposed method suitable for detecting the total amount of these most important biothiols in biological sample human plasma. Due to variations in the chemical composition of biological samples, a standard addition method was employed. Since Cys was the most abundant biothiol in human plasma, it was chosen to obtain the recovery of this method. The results are shown in Table S2, revealing that our method has great potential for quantitative analysis of thiols levels in practical samples. In addition, we have investigated the response of this biosensor to proteins with Cys residues such as bovine serum albumin (BSA), and found that the micromolecules like free thiol compound Cys were more sensitive than the macromolecules proteins with Cys residues (Fig. S10). We also investigated different reducing agents such as TCEP, ME, and DTT in biological samples preparation and found that TCEP was the best one because of the existence of thiol group in ME and DTT molecules (Fig. S11).

4. Conclusion

In summary, this study demonstrated a simple, sensitive, selective, and cost-effective fluorescence signal-off assay for the detection of biothiols based on the PEI-capped AgNCs. The quenching mechanism different from previous study was that the biothiols induced clusters agglomeration, leading to the formation of non-fluorescent nanoparticles. There were no quenching responses to other amino acids at ten-fold higher concentration than Cys, Hcy, and GSH, which permitted the detection of trace biothiols in biological fluids without the need of complicated sample pretreatment procedures. In addition, this assay could be simply visualized by the naked eyes without requirement of complicated instruments as the color changed from colorless to red-brown upon addition of biothiols. The successful detection of biothiols in human plasma samples suggested that the present method had great practicability for diagnostic purpose.

Acknowledgments

This work was supported by the National Natural Science Foundation of China (nos. 21273174, 20975083), the Municipal Science Foundation of Chongqing City (no. CSTC–2008BB 4013), and the 211 Project of Southwest University (the Third Term).

Appendix A. Supporting information

Supplementary data associated with this article can be found in the online version at http://dx.doi.org/10.1016/j.bios.2012.10.090.

References

Bistra, B., Valentin, L., Ivaylo, P.I., Antonia, T., Ivan, M., Vanio, M., 2008. Journal of Chromatography B 870, 103–108.
Cheng, W.L., Dong, S.J., Wang, E.K., 2003. Angewandte Chemie International Edition 42, 449–452.
Fletcher, A.N., 1969. Photochemistry and Photobiology 9, 439–444.
Gao, F., Ye, Q.Q., Cui, P., Chen, X.X., Li, M.G., Wang, L., 2011. Analytical Methods 3, 1180–1185.
Han, B.Y., Wang, E.K., 2011. Biosensors and Bioelectronics 26, 2585–2589.
Han, B.Y., Yuan, J.P., Wang, E.K., 2009. Analytical Chemistry 81, 5569–5573.
Henglein, A., Mulvaney, P., Linnert, T., 1991a. Faraday Discussions 92, 31–44.
Henglein, A., Mulvaney, P., Linnert, T., 1991b. Electrochimica Acta 36, 1743–1745.
Hong, R., Han, G., Fernández, J.M., Kim, B.J., Forbes, N.S., Rotello, V.M., 2006. Journal of the American Chemical Society 128, 1078–1079.
Huang, Y.F., Chang, H.T., 2006. Analytical Chemistry 78, 1485–1493.
Huang, Z.Z., Pu, F., Lin, Y.H., Ren, J.S., Qu, X.G., 2011. Chemical Communications 47, 3487–3489.
Kim, H., Namgung, R., Singha, K., Oh, I.K., Kim, W.J., 2011. Bioconjugate Chemistry 22, 2558–2567.
Lu, C., Zu, Y.B., Yam, V.W., 2007. Analytical Chemistry 79, 666–672.
Manoth, M., Manzoor, K., Patra, M.K., Pandey, P., Vadera, S.R., Kumar, N., 2009. Materials Research Bulletin 44, 714–717.
Moore, R.R., Banks, C.E., Compton, R.G., 2004. Analyst 129, 755–758.
Mulvaney, P., Linnert, T., Henglein, A., 1991. Journal of Physical Chemistry 95, 7843–7846.
Refsum, H., Ueland, P.M., Nygård, O., Vollset, S.E., 1998. Annual Review Medicine 49, 31–62.
Ruan, Y.B., Li, A.F., Zhao, J.S., Shen, J.S., Jiang, Y.B., 2010. Chemical Communications 46, 4938–4940.
Ruzi-Díaz, J.J.J., Torriero, A.A.J., Salinas, E., Marchevsky, E.J., Sanz, M.I., Raba, J., 2006. Talanta 68, 1343–1352.
Seshadri, S., Beiser, A., Selhub, J., Jacques, P.F., Rosenberg, I.H., D'Agostino, R.B., Wilson, P.W.F., Wolf, P.A., 2002. New England Journal of Medicine 346, 476–483.
Shahrokhian, S., 2001. Analytical Chemistry 73, 5972–5978.
Shahrokhian, S., Karimi, M., 2004. Electrochimica Acta 50, 77–84.
Shang, L., Dong, S.J., 2009. Biosensors and Bioelectronics 24, 1569–1573.
Shiu, H.Y., Wong, M.K., Che, C.M., 2011. Chemical Communications 47, 4367–4369.
Sun, S.K., Wang, H.F., Yan, X.P., 2011. Chemical Communications 47, 3817–3819.
Vosch, T., Antoku, Y., Hsiang, J.C., Richards, C.I., Gonzalez, J.I., Dickson, R.M., 2007. Proceedings of the National Academy of Sciences of the United States of America 104, 12616–12621.
Wang, P., Liu, J., Lv, X., Liu, Y.L., Zhao, Y., Guo, W., 2012. Organic Letters 14, 520–523.
Wlodek, L., 2002. Polish Journal of Pharmacology 54, 215–223.
Wood, Z.A., Schröder, E., Harris, J.R., Poole, L.B., 2003. Trends in Biochemical Sciences 28, 32–40.
Xu, H., Wang, Y.W., Huang, X.M., Li, Y., Zhang, H., Zhong, X.H., 2012. Analyst 137, 924–931.
Xu, H.X., Suslick, K.S., 2010. Advanced Materials 22, 1078–1082.
Zhang, Y., Li, Y., Yan, X.P., 2009. Analytical Chemistry 81, 5001–5007.
Zheng, J., Nicovich, P.R., Dickson, R.M., 2007. Annual Review of Physical Chemistry 58, 409–431.